

Focused resonance-enhanced mechanisms in atom-surface scattering

Salvador Miret-Artés

Instituto de Matemáticas y Física Fundamental, Consejo Superior de Investigaciones Científicas, Serrano, 123, 28006 Madrid, Spain

(Received 10 December 1998)

In recent years a number of resonance-enhanced mechanisms and focusing effects have been reported in inelastic atom-surface scattering. In this paper, we show that most of such scattering singularities are due to large values of the Jacobian (or density of states) of the incident momentum with respect to the final scattering angle leading to a unified theoretical scheme for their treatments. As a result, focused resonance-enhanced mechanisms are proposed and analyzed in order to improve the detection of bound states of low-index metal surfaces. [S0163-1829(99)10927-5]

The selective adsorption (SA) phenomenon in particle-surface scattering is currently being very actively investigated. Experimental detection of bound states is easily carried out with surfaces presenting a high corrugation allowing the construction of interaction potentials. However, for metal surfaces, detection of SA resonances is in general quite difficult and much effort is being devoted to choose carefully optimum experimental incident conditions to enhance resonance features. Several mechanisms have been predicted with this goal. Thus, for example, in elastic scattering, we have the so-called critical kinematic (CK) effect for atoms^{1,2} and diatomic molecules,³ which has been observed up to now only for diatomics. This effect takes place when a stationary value of the resonance curve (or kinematical resonance condition) equals the energy of a bound state. For inelastic scattering, additional resonance-enhanced mechanisms have been proposed and only some of them observed. The mechanism of phonon-assisted selective adsorption was first reported by Evans *et al.*⁴ and consists of a triple intersection of the resonance curve, a surface dispersion curve (typically the Rayleigh dispersion curve, RW) and the scan curve, which expresses the energy and momentum conservation laws. Alternatively, the focused inelastic resonance (FIR) mechanism is more adequate for the observation of the so far elusive bound states of atoms^{5,6} and diatomics⁷ on low-index metal surfaces. This mechanism occurs when the following two conditions in the energy transfer and parallel wave-vector exchange space are met: (i) the scan and resonance curves are tangent to each other for a particular bound state of the system and (ii) this tangency point belongs to the RW or any other surface or bulk phonon dispersion curve. The resulting kinematic equation is a condition for the final angle. A second important mechanism is the inelastic counterpart of the CK effect (ICK) predicted for atoms and diatomics although it has been observed so far for diatomics.⁷ Its kinematic condition is similar to that of the FIR effect but for the initial angle. In both mechanisms, the corresponding resonance features are easily observed in angular distributions due to the fact that the peaks remain in the same angular position for a given range of incident wave vectors. More resonance-enhanced mechanisms have been envisaged recently giving rise to some other effects.^{2,5} Very recently, a defect-mediated resonance mechanism has been also observed.⁸

On the other hand, in nonresonant scattering, two main inelastic focusing effects have been reported. The first one is the so-called kinematical focusing effect due to the vanishing of the Jacobian transforming momentum-space coordinates into angular coordinates.⁹ More recently, a scattering singularity called the inelastic focusing (IF) effect¹⁰ has also been identified and has its origin in the divergence in the Jacobian of the incident wave vector with respect to the final scattering angle. The IF occurs under special conditions in which the small spread of energies in the incident beam is sharply focused into a very narrow range of final angles. The corresponding mathematical condition is also valid for the *bunching* of the scan curves compatible with the incident parameters (angles and wave vectors) present in the incident beam and around the same value of phonon energy and momentum exchange. Finally, it has been observed that both singularities can occur at the same time as in the scattering of He atoms from the NaCl(001) surface.⁶

In this paper, we show that the IF effect can also be combined with the above-mentioned resonance-enhanced mechanisms leading to the best observation of bound states of atoms and molecules on low-index metal surfaces. In particular, in the light of these findings, the three FIR features recently observed in the scattering of D_2 molecules from the Cu(001) surface⁷ have been reexamined and a more complete theoretical interpretation is provided. For simplicity, only in-plane scattering will be considered but the final conclusions drawn will be valid for any general scattering event.

Due to the fact that the origin of most inelastic features can be understood from kinematics, the following kinematic equations can be taken as the starting point of our theoretical development (square wave-vector quantities will be given in energy units with $\hbar^2/2m = 1$, m being the mass of the incident particles):

diffraction condition (parallel momentum transfer),

$$\Delta K = k_f \sin \theta_f - k_i \sin \theta_i, \quad (1)$$

energy transfer

$$\Delta E = k_f^2 - k_i^2, \quad (2)$$

scan curve (SC)

$$\sin \theta_f = \frac{k_i \sin \theta_i + \Delta K}{\sqrt{k_i^2 + \Delta E}}, \quad (3)$$

resonance curve (RC) expressed in terms of the incident angle

$$\sin \theta_i = \frac{\sqrt{k_i^2 + \Delta E + |\epsilon_n|} - N - \Delta K}{k_i} \quad (4)$$

or as a function of the final angle

$$\sin \theta_f = \frac{\sqrt{|\epsilon_n| + k_i^2 + \Delta E} - N}{\sqrt{k_i^2 + \Delta E}}, \quad (5)$$

and the Rayleigh dispersion (RW) curve, which is usually written as

$$\Delta E = \pm \Delta E_{\max} \sin \frac{\pi \Delta K}{G}, \quad (6)$$

where k_f and k_i are the incident and final wave vectors of the particles, $\mathbf{N} = (\mathbf{N}_{\parallel}, \mathbf{N}_{\perp})$ is the two-dimensional reciprocal lattice vector exchanged in the resonance process with its parallel and perpendicular components to the scattering plane (this last component being set zero) and $|\epsilon_n|$ the n th bound state of the attractive interaction potential.

The total in-plane scattering intensity observed experimentally in angular distributions can be expressed in general in terms of integrals over the incident phase space and the angular acceptance of the detector of the total differential reflection coefficient written as¹⁰

$$\frac{dR(\mathbf{k}_f, \mathbf{k}_i)}{dE_f d\theta_f} = \frac{dR(\mathbf{k}_f, \mathbf{k}_i)}{dE_f dk_i} \frac{dk_i}{d\theta_f}. \quad (7)$$

The IF singularity occurs when the density of states of k_i in the final angular region becomes very large. In other words, when the factor $(d\theta_f/dk_i)_{SC}$ taken from the scan curve is equal to zero. The kinematic condition for such a singularity or bunching of SC's can be written as

$$\frac{k_i}{\sin \theta_i} = \frac{k_f}{\sin \theta_f} = \frac{\Delta E}{\Delta K} \quad (8)$$

and, along this paper, it will be emphasized that these ratios (we could consider them as fundamental ratios) play a very important role in the focused resonance-enhanced mechanisms analyzed. Moreover, the IF locus or parametric curve in the $(\Delta E, \Delta K)$ plane depending on k_i (keeping constant the final and incident angles) (Ref. 10)

$$\begin{aligned} \Delta E &= k_i^2 \frac{\sin^2 \theta_f - \sin^2 \theta_i}{\sin^2 \theta_i} \\ \Delta K &= k_i \frac{\sin^2 \theta_f - \sin^2 \theta_i}{\sin \theta_i} \end{aligned} \quad (9)$$

can be shown to be tangent to the bunching of SC's. We also notice that from the derivatives of ΔE and ΔK with respect to k_i , the IF-locus slope is given by

$$\frac{d\Delta E}{d\Delta K} = 2 \frac{k_i}{\sin \theta_i}. \quad (10)$$

The observation of the IF effect requires that the point of tangency corresponds to some excitation (with preference a surface one). In general, the region of concatenation between the IF locus and the bunching of SC's is quite extended and the focusing condition is fulfilled for a wide range of k_i values.¹⁰ Thus, the IF peaks are easy to recognize in angular distributions since they are also placed at *constant angular positions* for those k_i values.

Our goal now is to analyze the feasibility of combining the IF singularity with the FIR and ICK mechanisms for an even better observation of bound states on low-index metal surfaces:

(i) *FIR mechanism plus IF*: An alternative derivation of the FIR effect can be easily reached from Eq. (5) by calculating the derivative $(d\theta_f/dk_i)_{RC}$ and setting it equal to zero. Doing this, we can then write the FIR condition as follows

$$\frac{k_f}{\sin \theta_f} = \frac{N}{\cos^2 \theta_f} = \frac{|\epsilon_n|}{N} \quad (11)$$

and the corresponding FIR locus as⁵

$$\begin{aligned} \Delta E &= -k_i^2 + \frac{|\epsilon_n| [|\epsilon_n| - N^2]}{N^2} \\ \Delta K &= -k_i \sin \theta_i + \frac{|\epsilon_n| - N^2}{N}. \end{aligned} \quad (12)$$

Now by equating the IF locus, Eq. (9), and the FIR locus, Eq. (12), we have that

$$\frac{k_f}{\sin \theta_f} = \frac{|\epsilon_n|}{N} = \frac{\Delta E}{\Delta K} = \frac{k_i}{\sin \theta_i} \quad (13)$$

thus, whenever this relation holds both effects can be fulfilled at the same time in the resonant scattering. Furthermore, the FIR-locus slope can be shown to be equal to Eq. (10) and therefore, an extended region of concatenation between both loci (FIR and IF) can be found. When Eq. (13) is fulfilled, a very simple pictorial way to estimate the RW phonon magnitudes (ΔE and ΔK) exchanged in the resonant scattering is readily obtained from Eq. (6), namely

$$\frac{|\epsilon_n|}{N} = \pm \frac{\pi \Delta E_{\max}}{G} \frac{\sin(\pi \Delta K/G)}{(\pi \Delta K/G)} \quad (14)$$

where the right-hand side is similar to a typical diffraction function taking ΔK as independent variable. The crossings of the constant ratios (one for each bound state) with that function will give us the corresponding ΔK values. A further enhancement is expected if a given ratio is tangent to some of the extrema displayed by the diffraction function because in this case the density of phonon states is specially very high.

(ii) *ICK mechanism plus IF*: due to the fact that the ICK effect is a condition for the incident angle we can readily obtain from Eq. (4) the derivative $(d\theta_i/dk_i)_{RC}$ and equate it to zero leading to the following ICK condition

TABLE I. Rotational bound states (in meV) labeled by (n,J) , experimental FIR angles (in degrees), and the corresponding ratios $|\epsilon_{n,J}|/N$ and final wave vectors (in \AA^{-1}) for the scattering of D_2 from Cu(001). The reciprocal lattice vector exchanged in the resonance process is $\mathbf{N}=(3.48,0)$ (\AA^{-1}). The incident angle is obtained from $\theta_f + \theta_i = 95.76^\circ$ due to the geometry used in the experimental setup (Ref. 7).

(n,J)	$ \epsilon_{n,J} $ (meV)	θ_f^{FIR}	$ \epsilon_{n,J} /N$ (\AA^{-1})	k_f (\AA^{-1})
(3,0)	10.3	38.6	5.70	3.56
(1,1)	12.4	44.5	6.87	4.82
(0,1)	21.5	57.3	11.91	10.02

$$\frac{k_i}{\sin \theta_i} = \frac{\Delta E + |\epsilon_n|}{\Delta K + N} = \frac{\Delta K + N}{\cos^2 \theta_i}. \quad (15)$$

The ICK locus is now expressed as

$$\Delta E = -|\epsilon_n| + k_i^2 \frac{\cos^2 \theta_i}{\sin^2 \theta_i}$$

$$\Delta K = k_i \frac{\cos^2 \theta_i}{\sin \theta_i} - N \quad (16)$$

and the slope of the ICK locus is again the same as given by Eq. (10). Furthermore, by equating both loci (ICK and IF) we recover Eq. (13). In most of experimental setups, the incident and final angles are related by the following geometrical expression $\theta_i + \theta_f = \theta_{SD}$, with θ_{SD} being a fixed angle between the beam source and the detector and, therefore, $d\theta_i/d\theta_f = -1$. A very interesting focused resonance-enhanced mechanism could then be possible: the ICK effect for the initial angle and the FIR effect for the final angle at IF conditions. In this special case, a very high intensity is expected to be observed. Similar final conclusions are reached for the CK effect doing $\Delta E = \Delta K = 0$ in Eq. (15). In this way, and comparing with the FIR condition, Eq. (11), it is possible to envisage a combination of FIR and CK or vice-versa in a resonant scattering event. This new mechanism has already been observed in the D_2 scattering from Cu(001).⁷

Recently, in the resonant scattering of D_2 from the Cu(001) surface three FIR peaks have been observed and assigned to the rotational levels $(n,J)=(3,0),(1,1),(0,1)$ with values 10.3, 12.4, and 21.5 meV, respectively⁷ (see Table I). In this case, the formulation above described remains valid when replacing $|\epsilon_n|$ by $|\epsilon_{n,J}|$ with $|\epsilon_{n,J}| = |\epsilon_n| - B_{rot}J(J+1)$, B_{rot} being the diatomic rotational constant. The k_i values used in the experiment covered the range $5.55\text{--}7.60 \text{\AA}^{-1}$. In Fig. 1, Eq. (14) is plotted to show if some of the FIR features observed can be also attributed to the IF singularity. The horizontal lines are the ratios listed in Table I and the different crossings with the two curves give possible ΔK values, which could be exchanged in the resonant process involved. For the first two resonances, (3,0) and (1,1), the horizontal lines 5.70 and 6.87\AA^{-1} , respectively, are also nearly tangent to the second maximum displayed by the diffractiontype function. Obviously, in order to know if these ΔK values are accessible with the requirements imposed by the FIR condition, we have to build the IF, FIR, and ICK loci keeping constant the incident and final angles

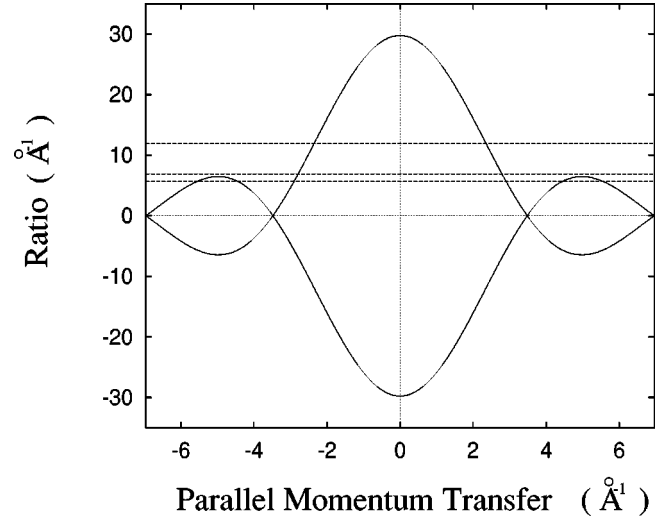


FIG. 1. Equation (14) is depicted as a function of the parallel momentum transfer ΔK . The horizontal lines are the ratios listed in Table I with values 5.70 , 6.87 , and 11.91\AA^{-1} from bottom to top.

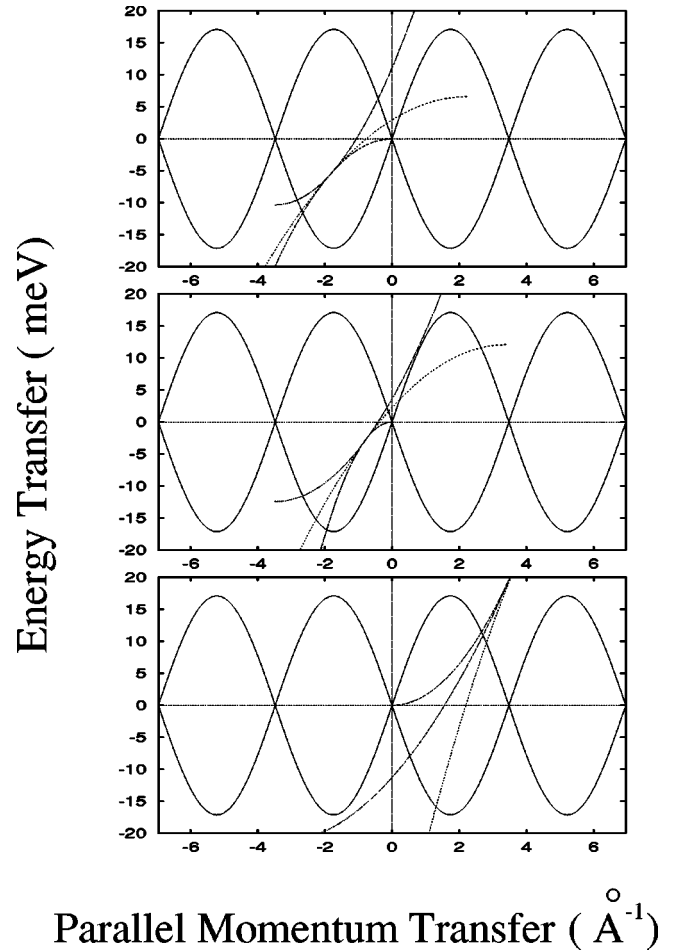


FIG. 2. In the $(\Delta E, \Delta K)$ plane, the RW dispersion curves (solid lines), the IF locus (dashed semiparabola with vertex in the origin of coordinates), the FIR locus (small-dashed semiparabola) and the ICK locus (dotted semiparabola) are plotted for the (3,0), (0,1), and (0,1) resonances in the scattering of D_2 from Cu(001) from top to bottom, respectively.

at their FIR values and running over a wide range of incident wave vectors, for example between 0 and 10 \AA^{-1} . In Fig. 2 (from top to bottom), the corresponding plots are shown for the (3,0), (1,1), and (0,1) resonances, respectively. The RW dispersion curves are sine functions (solid lines), the IF locus is represented by a dashed semiparabola with vertex in the origin of coordinates, the FIR locus by a small-dashed semiparabola and the ICK locus by a dotted one. On top of Fig. 2, the crossing of the FIR locus with the RW curve within the creation region indicates the presence of a FIR feature in the angular distribution within the range of incident wave vectors above indicated. In the same region, the IF and FIR loci nearly coincide in a quite extended zone very near to the RW phonon. This concatenation takes place only in the first zone for $\Delta K \sim -3 \text{ \AA}^{-1}$ and, in Fig. 1, the first crossing of the lowest horizontal line is also around the same value of ΔK . On the contrary, for the second resonance (middle of Fig. 2) and for the k_i values covered by the experiment, the FIR occurs within the annihilation region very near to $\Delta K \sim 0$. Comparing with the several crossings observed in Fig. 1, for the second horizontal line, small ΔK values cannot be reached with the conditions imposed by the FIR mechanism. Concerning the (0,1) resonance (bottom of Fig. 2), the region of concatenation of both loci is situated at very high-phonon energies, in the transition from the first to the second zone and for k_i values comprised between $7.4\text{--}8.0 \text{ \AA}^{-1}$. The ratio 11.91 \AA^{-1} cuts the diffractiontype function only in the first zone for $\Delta K \sim -2.5 \text{ \AA}^{-1}$. So we can finally conclude that only the first resonance could be considered as due to a focused resonance-enhanced mechanism.

So far, no mention to the ICK locus has been done. Regions of concatenation of the three loci, for the same range of

k_i values, are also possible. This fact is clearly seen on the bottom of Fig. 2 but the phonons participating in such a process are not surface phonons and the corresponding feature should be very weak. On the other hand, from the middle of Fig. 2, the ICK locus is nearly tangent to the RW dispersion curve in the annihilation region for k_i values between $7.8\text{--}9 \text{ \AA}^{-1}$. This would correspond again to a very singular resonance process where a ICK feature should be observable at constant angular position. Unfortunately, for $k_i > 7.0 \text{ \AA}^{-1}$, rotational inelastic diffraction peaks begin to appear masking therefore, for this system, any further singular resonance feature. In turn, a very interesting resonance-enhanced mechanism can again be predicted when the FIR or ICK locus are tangent to a RW dispersion curve for a large range of k_i values.

In all of the cases undertaken in this paper, we have demonstrated that the focused resonance-enhanced mechanisms analyzed arise from the singularity of the density of states of k_i in the final or initial angular region. The corresponding kinematic relations found can be written in a very simple way in terms of the so-called fundamental ratios. We have put in evidence that the inclusion of the main characteristics of the incident beam (energy and angular resolution) has a substantial effect in the searching for optimum conditions to make weak-resonance features observable. Due to the fact that the entire narrow energy distribution of the incident beam is focused in a given final direction, the corresponding focused resonance peaks are unaffected by the energy broadening of the beam leading to sharp and quite distinctive signatures.

This work has been supported by DGICYT under Contract No. PB95-0071.

¹M. Hernández, S. Miret-Artés, P. Villarreal, and G. Delgado-Barrio, *Surf. Sci.* **251/252**, 369 (1991); **21**, 274 (1992); S. Miret-Artés, *ibid.* **141**, 294 (1993).

²S. Miret-Artés, *Surf. Sci.* **366**, L735 (1996).

³M. F. Bertino, S. Miret-Artés, and J. P. Toennies, *Chem. Phys. Lett.* **287**, 663 (1998).

⁴D. Evans, V. Celli, G. Benedek, J. P. Toennies, and R. B. Doak, *Phys. Rev. Lett.* **50**, 1854 (1983).

⁵G. Benedek and S. Miret-Artés, *Surf. Sci. Lett.* **339**, L935 (1995).

⁶G. Benedek, R. Gerlach, A. Glebov, G. Lange, S. Miret-Artés, J. G. Skofronick, and J. P. Toennies, *Phys. Rev. B* **53**, 11 211 (1996).

⁷M. F. Bertino, S. Miret-Artés, J. P. Toennies, and G. Benedek, *Surf. Sci.* **377–379**, 714 (1997); *Phys. Rev. B* **56**, 9964 (1997).

⁸A. Glebov, J. R. Manson, J. G. Skofronick, and J. P. Toennies, *Phys. Rev. Lett.* **78**, 1508 (1997).

⁹G. Benedek, *Phys. Rev. Lett.* **35**, 234 (1975).

¹⁰A. Glebov, J. R. Manson, S. Miret-Artés, J. G. Skofronick, and J. P. Toennies, *Phys. Rev. B* **57**, R9455 (1998).